NUMERICAL STUDY ON THE NATURALLY CAPTURED AIR VOLUME OF OUTSIDE CABIN HEAT EXCHANGER FOR WIND POWER GENERATION

by

Nianyong ZHOU [a*]***, Yixing GUO*** [a]***, Wenbo LIU*** [a]***, Hao FENG*** [a]***, Haoping PENG*** [a*]***, Yun LEI*** [a]***, Song DENG*** [a]***, and Lei ZHAO*** [b]

[a] School of Petroleum Engineering, Changzhou University, Changzhou, Jiangsu, China
[b] Avic Xinxiang Aviation industry (Group) Co., LTD., Xinxiang, Henan, China

Original scientific paper
https://doi.org/10.2298/TSCI220123066Z

In this paper, the outside cabin heat exchanger based on the porous media approach was established. The effects of altitude, viscous resistance coefficient, inertial resistance coefficient, and core thickness on the naturally captured air volume of the heat exchanger were investigated by numerical simulation. Results showed that the naturally captured air volume of the heat exchanger tends to be larger on both sides and smaller in the middle, and there is a quasi-linear increase proportional to the incoming wind velocity. With the increment of altitude, viscous resistance coefficient, and inertial resistance coefficient, the average naturally captured air volume of the heat exchangers shows a downward trend. The trend would be clear with the increment of the incoming wind velocity, nevertheless, the effect of core thickness is weak. In addition, the design values of the viscous resistance coefficient and the inertial resistance coefficient should be restricted in the order of 10^6 *and below 500, respectively. Based on the weak effect of the naturally captured air volume of the heat exchanger, the thickness of the core can be appropriately increased to ensure the heat transfer area of the heat exchanger.*

Key words: *wind power generation, outside cabin heat exchanger, naturally air captured, porous media theory*

Introduction

With the decrease of wind power subsidies year after year, the wind power industry is not only developing towards high power models but also towards low cost and high stability. The wind power cooling system is a critical component to ensure the stable operation of power generation. Effectively improving the heat transfer capacity and reliability of the cooling system is highly concerning in the wind power field. Nowadays for outside cabin heat exchanger with a water cooling system for wind power generation, the natural air captured cooling is used to replace the traditional fan-forced wind cooling and liquid cooling. The installation of fans and other equipment is avoided. The manufacturing and operation costs of the cooling system are reduced. Meanwhile, it has the advantages of simple structure, convenient management and maintenance. The reliability of the cooling system is effectively improved.

The naturally captured air volume plays an important role in the heat transfer performance of the outside cabin heat exchanger. However, considering the complex core structure for

* Corresponding authors, e-mail: zhounianyong@cczu.edu.cn, php@cczu.edu.cn

the heat exchanger, it is difficult to directly establish the real model and perform simulation. It is a common method for scholars to simplify the heat exchanger model by porous media. Patankar and Spalding [1] first introduced the method of porous media to replace the heat exchanger and numerically simulated it. Some researchers [2-5] used a porous media model to simulate the pressure drop and heat transfer performance of the heat exchanger. In the process of numerical simulation, the pressure drop of the heat exchanger was usually used as a reference. On this basis, the error of pressure drop results obtained by experiment and numerical simulation was acceptable in a certain range. Therefore, the feasibility of the porous media model was verified. Vlahostergios *et al.* [6] investigated experimentally the influence of the turbulence intensity on the heat transfer performance and pressure drop of the heat exchanger. It was found that with the increase of turbulent intensity, the total outflow pressure drop of the heat exchanger decrease and the heat transfer capacity is enhanced. The model of tube and belt heat exchanger was established using the porous media method by Guo *et al.* [7]. The fin opening and spacing were analyzed by numerical simulation, and the optimal heat transfer and resistance characteristics of the heat exchanger were obtained. The effects of dynamic viscosity and incoming wind velocity on volume distribution and pressure drop of the plate-fin heat exchanger were investigated through the porous media method [8-11]. Results showed that the volume distribution of the heat exchanger becomes more uniform and the pressure drop decreases with the increase of dynamic viscosity. Some investigators [12-14] analyzed the effects of porosity and permeability on heat transfer efficiency and pressure drop of shell and tube heat exchanger. Results showed that when the porosity and permeability are 0.2 and 10^{-9} m^2, respectively, the optimal heat transfer performance and smaller pressure drop of shell and tube heat exchanger can be obtained. Qu *et al.* [15] and Yan [16] found that the pressure drop at the inlet and outlet of the heat exchanger tends to be directly proportional to the thickness. The increase of core thickness has little effect on the heat transfer performance of the heat exchanger. Isik and Tugan [17] used the CFD method to study the influence of baffle cut on heat transfer performance and pressure drop of shell and tube heat exchange. It was found when the baffle cut rate is 40% and 20%, the highest and the lowest heat transfer per pressure drop for the shell and tube heat exchanger are achieved, respectively. Tang *et al.* [18] analyzed the effect on heat transfer and pressure drop of the heat exchanger between different inlet angles by experimental and numerical methods. Results showed that the optimal and the worst overall heat transfer performance of the heat exchanger can be obtained when the air inlet angle is 45° and 30°. The influences of altitude and incoming wind velocity on heat transfer performance and the naturally captured air volume of the heat exchanger were analyzed [19-21]. It was found that with the decrease of altitude, the heat transfer performance of the heat exchanger is further enhanced, and the pressure drop and the naturally captured air volume of the heat exchanger are also increased.

In conclusion, the aforementioned researches mainly focus on the heat transfer performance and pressure drop characteristics of the heat exchanger. However, there are few studies on the air captured capacity of the heat exchanger in the natural wind field. Therefore, given the shortcomings of the existing research, the numerical model of the outside cabin heat exchanger of wind power generation based on porous media was established. The effects of altitude, viscous resistance coefficient, inertial resistance coefficient, and core thickness on the air captured capacity of outside cabin heat exchanger in natural wind field were analyzed. Results can provide theoretical and data support for the performance improvement of the wind power cooling system and optimization of the heat exchange, which has significance in engineering and application fields.

Model set-up

Physical model

In this paper, the physical model is an outside cabin heat exchanger with a plate-fin structure of a 4.5 MW wind power generation. As shown in fig. 1, the air side channel of the heat exchanger adopts wavy fins. The overall length, thickness, and width of the single heat exchanger are 2110 mm, 94 mm, and 550 mm, respectively. The air side has channels with 41 layers. The ethylene glycol solution side has channels with 40 layers. The air and ethylene glycol working fluid-flow along the length direction of the channel. In addition, the thickness of the intermediate partition wall on the air side and ethylene glycol side is 0.8 mm.

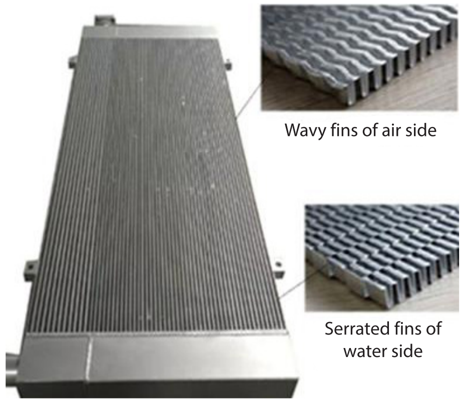

Figure 1. The single module of outside cabin heat exchanger

The outside cabin heat exchanger of a 4.5 MW wind power generation is arranged on the top of the engine room. Seven single heat exchangers with the same structure size are assembled on the support frame. The generator and the gearbox are each cooled by three heat exchangers, respectively, and the converter is cooled by another one.

Simplification of the physical model

Considering the relatively complex structure of the outside cabin heat exchanger, it is difficult to model its real physical size. In this paper, the porous media model was adopted to simplify the heat exchanger. The fluid-flow in the heat exchanger is characterized by setting resistance parameters in the porous media region. In the process of studying the naturally captured air volume of the outside cabin heat exchanger, considering the infinite boundary condition of the natural wind field, a suitable numerical model of the natural wind field around the heat exchanger was established, as shown in fig. 2. The size of the natural wind field is length, L = 36.4 m, width W = 13.5 m, and height H = 6 m, respectively.

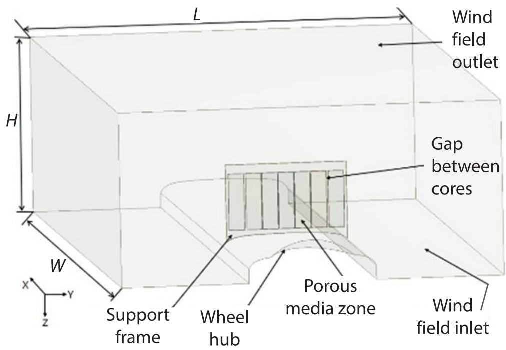

Figure 2. Heat exchanger simulation model in the natural wind field

Mathematical model

Governing equation

Continuity equation:

$$\frac{\partial u_i}{\partial x_i} = 0 \tag{1}$$

where u [ms^{-1}] is the velocity of the fluid and x represents the space co-ordinate.

Momentum equation of porous media:

$$\frac{\partial (u_i u_j)}{\partial x_j} = -\frac{1}{\rho}\frac{\partial p}{\partial x_i} + \frac{1}{\rho}\frac{\partial}{\partial x_j}\mu_{\text{eff}}\left(\frac{\partial u_i}{\partial x_j} + \frac{\partial u_j}{\partial x_i}\right) \tag{2}$$

where subscripts i and j are directions, p [Pa] is the static pressure, μ_{eff} [Pa·s] – the effective viscosity of the fluid, and ρ [kgm^{-3}] – the density of the fluid.

The porous media model is based on the momentum equation with the addition of the source term:

$$S_i = -\left(\sum_{j=1}^{3} D_{ij} \mu u_j + \sum_{j=1}^{3} C_{ij} \frac{1}{2} \rho |u| u_j \right) \tag{3}$$

On the right side of eq. (3), the first term and the second term represent the viscous loss term and the inertial loss term, respectively, where S_i [kgm^{-2}s^{-2}] is the momentum source term in i^{th} direction, μ [Pa·s] – the dynamic viscosity of the fluid, u_j [ms^{-1}] – the face velocity for the j^{th} (x, y, or z) direction, |u| [ms^{-1}] – the magnitude of the velocity, and D_{ij} and C_{ij} are the viscous loss coefficient matrix and the inertial loss coefficient matrix, respectively. Considering that the flow direction of the natural wind in the heat exchanger is 1-D, eq. (3) can be simplified:

$$S_i = -\left(\frac{\mu}{\alpha} u_j + C_2 \frac{1}{2} \rho |u| u_j \right) \tag{4}$$

where α [m^2] is the permeability, the $1/\alpha$ can be set as C_1 [m^{-2}] – the viscous resistance coefficient, and C_2 [m^{-1}] – the inertial resistance coefficient.

For porous media, the source term acting on the fluid produces a pressure gradient, and the pressure drop in the direction of the fluid-flow can be expressed:

$$\Delta P = S_i \Delta n \tag{5}$$

where ΔP [Pa] is the pressure drop and Δn [mm] – the porous media thickness.

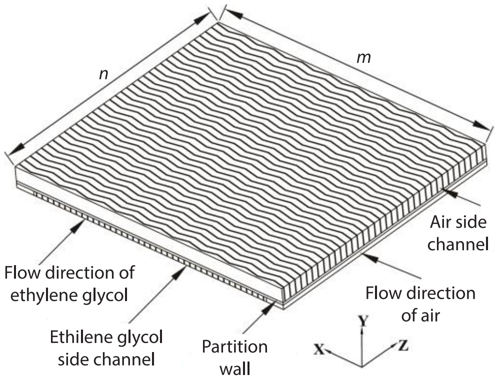

Figure 3. Heat exchanger unit model

Table 1. Numerical simulation values of wind velocity and pressure drop in heat exchanger unit

Wind velocity [ms^{-1}]	Pressure drop [Pa]
1.5	34
2	49
2.5	66
3	89
3.5	116
4	145

Determination of C1 and C2 of porous media

In this study, the finned structure of the heat exchanger is arranged periodically. Thus, a section of the heat exchanger can be used as the heat exchanger unit for simulation. In the heat exchanger unit, the length of the air side channel is selected as the total air channel length (m = 94 mm) and the length of the ethylene glycol solution side channel is selected as the unit length (n = 80 mm).

Considering the symmetry of the heat exchanger core structure, a half air channel and half ethylene glycol solution channel were used in the heat exchanger unit geometry model in the height direction. The air and the glycol solution flow in a crossflow direction, as shown in fig. 3.

The pressure drop of the heat exchanger unit model under different incoming wind velocities can be calculated by simulating the heat exchanger unit model. The specific values of the simulation are shown in tab. 1.

The aforementioned simulated values of wind velocity and pressure drop measured were fitted in the form of the quadratic polynomial of $\Delta P = au^2 + bu$, and the fitting results were expressed:

$$\Delta P = 5.33u^2 + 12.33u \tag{6}$$

Simultaneous eqs. (4)-(6), and the following relationship can be obtained by comparing and correlating the previous equations:

$$a = \frac{1}{2}C_2\rho\Delta n = 5.93,\ \ b = \frac{\mu}{\alpha}\Delta n = 12.33 \tag{7}$$

where a and b represent fitting coefficients, μ was taken as $1.7894 \cdot 10^{-5}$ Pa·s, ρ was taken as 1.225 kg/m^3, and Δn was taken as 94 mm. The aforementioned parameters were put into eq. (7), C_1 and C_2 were calculated as $7.33 \cdot 10^6$ and 10^3, respectively.

Boundary conditions and parameter settings

In the process of numerical simulation, the velocity inlet boundary was adopted. In the natural wind field of the actual power generation, the incoming wind velocity was generally graded 3-8 wind (5-20 m/s). The natural wind field outlet was set as the pressure outlet boundary. Both sides and upper areas of the natural wind field were set as the symmetrical boundary, and the bottom was set as the wall boundary. For the heat exchanger core, the porous zone with the laminar flow was adopted. The values of C and C_2 were set in the porous media region. The air-flow in the heat exchanger does not consider the effect of mutual intersection, so only the coefficient value of X air-flow direction was given.

In addition, the standard κ-ε model with the wall function was adapted for turbulent modelling. Pressure-based SIMPLEC algorithm and upwind second-order were utilized for coupling between velocity and pressure and discretizing parameters, respectively.

Verification of mesh independence and porous media method

To ensure the accuracy of model simulation results, models with grid numbers of 1.26 million, 1.6 million, 1.9 million, 2.16 million, and 2.46 million were established, respectively. When the wind velocity of the natural wind field was 10 m/s, the average inlet and outlet pressure drop, as well as the average naturally captured air volume of the single heat exchanger, were taken as reference quantities to verify the grid independence, as shown in fig. 4. When the number of grids was restricted at about 1.9 million, the numerical results of the two groups of selected reference quantities tended to be stable. Therefore, the model with 1.9 million grids was selected in this paper.

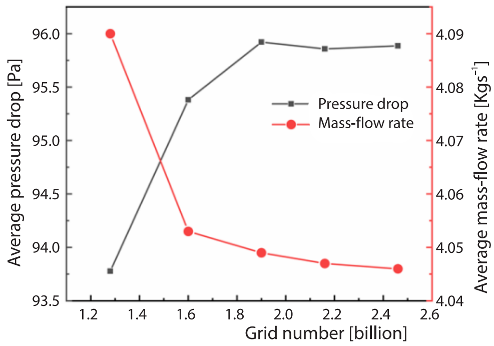

Figure 4. Grid independence verification curve

To verify the accuracy of the method based on the porous media model, the experimental platform for the naturally captured air volume of the outside cabin heat exchanger was built. When the heat exchanger was located at a height of 1400 m, the average naturally captured air volume of the single heat exchanger was determined under different incoming wind velocities. The experimental and simulation results obtained were shown in tab. 2. It was found that the experimental results are consistent with simulation results under different incoming wind velocities. When the incoming wind velocity is 6.76 m/s, the maximum error between them is about 9%, which meets the requirements of engineering calculation. As a result, it was feasible to investigate the natural wind capture of the heat exchanger based on the porous media model.

Table 2. The error between experimental and simulated data about the average naturally captured air volume of the single heat exchanger

Incoming wind velocity [ms^{-1}]	Experimental data [kgs^{-1}]	Simulated data [kgs^{-1}]	Error [%]
4.49	0.967	1.049	-8.49
5.59	1.472	1.475	-0.23
6.76	2.171	1.972	9.17
7.69	2.466	2.368	3.97
8.81	2.842	2.996	-5.42
9.79	3.259	2.260	0
11.49	3.979	3.656	8.14

The errors of experimental measurement and numerical simulation are mainly caused by the following two reasons. One reason is that the simulation model was appropriately simplified, as well as the deviation induced by formula fitting while solving the relevant resistance coefficients. Another reason is the deviation brought by the experimental measurement in the external environment.

Results and discussion

Flow field analysis of naturally air captured of outside cabin heat exchanger

When the incoming wind velocity in the natural wind field was 10 m/s, the heat exchanger with the core thickness of 94 mm and altitude at 0 m was simulated. By selecting the calculation model along the *X*-direction central section and the heat exchanger core along the *Y*-direction central section, the pressure and velocity nephograms were analyzed.

As shown in fig. 5, when the air-flow through the heat exchanger, due to the obstruction of the heat exchangers, the flow velocity of the air above the heat exchangers increases gradually, while the flow velocity of air behind the heat exchanger decreases gradually. The wind velocity decreases in the local area behind the heat exchanger due to the backflow disturbance. In addition, from figs. 6 and 7, it can be found that the velocity and pressure drop dis-

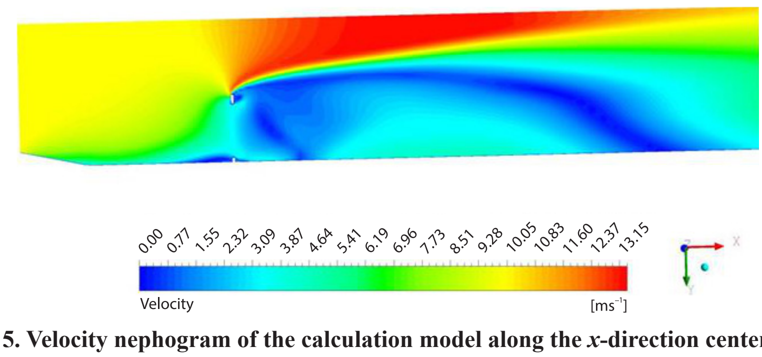

Figure 5. Velocity nephogram of the calculation model along the *x*-direction center section

tribution of the seven single heat exchangers in the natural wind field shows the trend of larger on both sides and smaller in the middle. The heat exchangers on both sides are comparatively stronger in terms of air captured capacity, whereas the middle portion is considerably weaker.

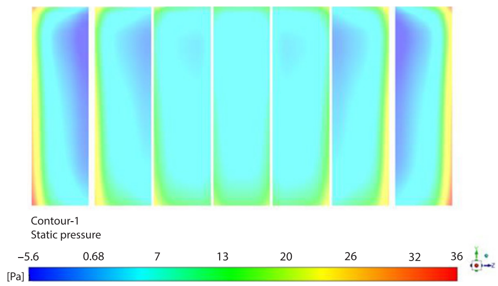

Figure 6. Pressure nephogram of the heat exchanger along the *Y*-direction center section

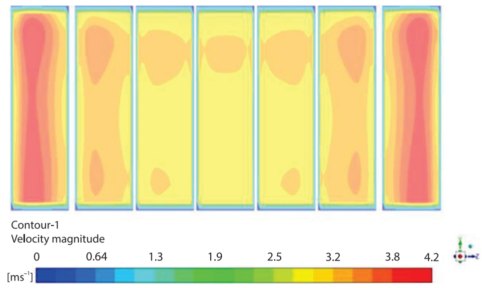

Figure 7. Velocity nephogram of the heat exchanger along the *Y*-direction center section

Influence of altitude on air captured capacity of the heat exchanger

The changes in physical parameters such as air pressure, density, and dynamic viscosity caused by altitude in different regions will further affect the air captured capacity of the heat exchanger. Maintain the parameters of the heat exchanger core thickness C_1 and C_2 unchanged. By changing the physical characteristics of the air, the effect of altitude on the naturally captured air volume of the heat exchanger was studied.

As shown in fig. 8, the average naturally captured air volume of the single heat exchanger increases with the increasing incoming wind velocity at different altitudes, showing a quasi-linear relationship. When the altitude is 0 m, the average naturally captured air volume of the single heat exchanger grows by 1.2 kg/s for every 2.5 m/s increase in incoming wind velocity. Under the same incoming wind velocity, the naturally captured air volume of the heat exchanger decreases gradually with the altitude increasing. The effect of altitude becomes more noticeable as the incoming wind velocity increases. This phenomenon is particularly significant when the altitude rises from 0-1400 m, which is mainly caused by the great change in air density. When the altitude ranges from 1400-4400 m, the reduction of the heat exchanger's naturally captured air volume is similar for every 1000 m increase, which is also due to the relatively uniform reduction in air density. When the incoming wind velocity reaches 10 m/s, the average naturally captured air volume of the single heat exchanger at an altitude of 4400 m is 2.16 kg/s lower than that at an altitude of 0 m, with a reduction range of roughly 1.7%.

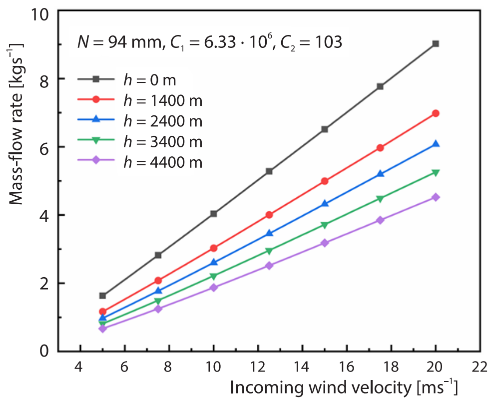

Figure 8. Variations of the average naturally captured air volume with incoming wind velocity at different altitudes

Influence of C_1 on air captured capacity of the heat exchanger

According to eqs. (3) an (4), the fluid-flow resistance in porous media depends on viscous resistance and inertial resistance. The C_1 and C_2 reflect the viscosity loss and inertial loss of fluid-flowing in porous media, respectively to a certain extent. Many researchers [22-25] showed that C_1 and C_2 are geometric characteristic parameters of porous media, which describe the difficulty of fluid-flowing through porous media. They are related to the pore structure of porous media such as porosity and tortuosity. The pore structure is embodied in the flow channel shape and fin type of heat exchanger. To investigate the influence of the pore structure of porous media on the air captured capacity of the heat exchanger, the core thickness and altitude parameters of the heat exchanger were kept unchanged during the simulation, and C_1 and C_2 were analyzed separately. Initially, the influence of C_1 was studied, in which the values of C_1 were taken as $7.33 \cdot 10^5$, $7.33 \cdot 10^6$, $4.03 \cdot 10^7$, and $7.33 \cdot 10^7$, respectively.

As illustrated in fig. 9, on the whole, with the increase of the C_1, the air captured capacity presents a downward trend. The downward tendency becomes more obvious as the incoming wind velocity increases. When values of C_1 are $7.33 \cdot 10^5$ and $7.33 \cdot 10^{6,}$ respectively, there is a quasi-linear relationship between the average captured air volume of the heat exchanger and the incoming wind velocity. When values of C_1 are $4.03 \cdot 10^7$ and $7.33 \cdot 10^7$, respectively, there is a parabolic relationship between the average captured air volume of the heat exchanger and the incoming wind velocity. At the same incoming wind velocity, the captured air volume of the heat exchanger decreases with the increase of C_1. The captured air volume of the heat exchanger decreases significantly as the C_1 is increased from $7.33 \cdot 10^6$ to $7.33 \cdot 10^7$.

In order to fully investigate the influence of C_1 on air captured capacity of the heat exchanger, the value range of C_1 was appropriately expanded. Several appropriate C_1 were selected to analyze the naturally captured air volume of the heat exchanger when the incoming wind velocity was 10 m/s.

As shown in fig. 10 as the value of C_1 gradually increases from 10^3 to $7.33 \cdot 10^5$, the naturally captured air volume of the single heat exchanger almost does not vary with the growth of C_1 and remains stable around 5.08 kg/s. The naturally captured air volume of the heat exchanger decreases exponentially with the rise of C_1 when the value of C_1 is between $7.33 \cdot 10^6$ and $7.33 \cdot 10^8$. When the value of C_1 continues to increase to $7.33 \cdot 10^8$, it also reaches

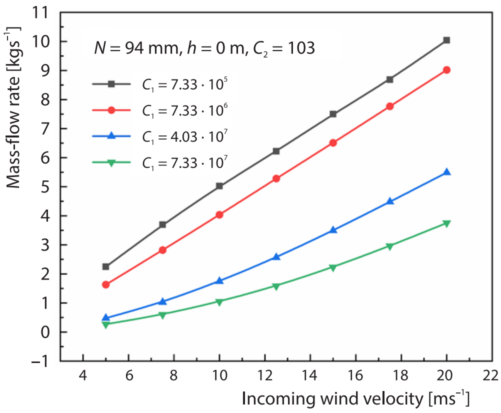

Figure 9. Variations of the average naturally captured air volume with incoming wind velocity at different viscous resistance coefficient

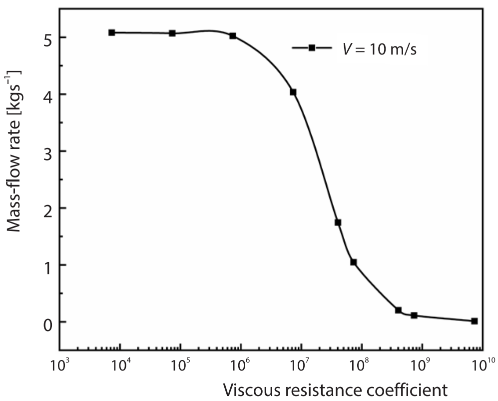

Figure 10. Variations the average naturally captured air volume with viscous resistance coefficients

the critical state. After that, the naturally captured air volume of the single heat exchanger gradually declines to 0 kg/s with the increase of C_1. As a result, for the naturally captured air volume of the heat exchanger, it is generally recommended that the design value of C_1 is restricted at the order of magnitude of 10^6, the air captured effect is relatively better at this time.

Influence of C_2 on air captured capacity of the heat exchanger

Similarly, when the values of the C_2 were set to 0, 103, 1030, and 2060, respectively, the air captured capacity of the heat exchanger was investigated in this paper.

As illustrated in fig. 11, on the whole, with the increase of the C_2, the air captured capacity presents a downward trend. With the increase of incoming wind velocity, the downward tendency is more apparent. There is a quasi-linear relationship between the average captured air volume of the heat exchanger and the incoming wind velocity, which is different from C_1. As the value of C_2 is 2060, each increment in incoming wind velocity in the natural wind field is 2.5 m/s, and the naturally captured air volume of the single heat exchanger is increased by 0.3 kg/s. Compared with the value of C_2 is 103, the air captured capacity of the heat exchanger is poor. When the inertial resistance is not considered, this means that the value of C_2 is 0. With the increase of the incoming wind velocity, it can be found that the naturally captured air volume of the heat exchanger shows a dramatically increase trend.

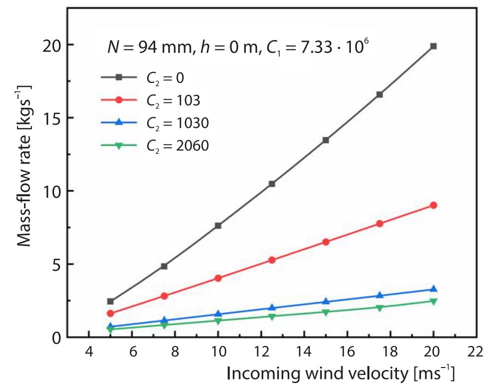

Figure 11. Variations of the average naturally captured air volume with incoming wind velocity at different inertial resistance coefficient

To further analyze the influence of C_2 based on keeping the incoming wind velocity at 10 m/s constants, an appropriate numerical range of C_2 was selected to analyze the naturally captured air volume of the heat exchanger.

As shown in fig. 12, as the value of C_2 increases from 0-500, the air captured capacity of the heat exchanger decreases rapidly. As C_2 continues to increase, the naturally captured air volume of the heat exchanger steadily declines and becomes stable. The value of C_2 after 1000 has little effect on the air captured capacity of the heat exchanger. Therefore, for the naturally captured air volume of the heat exchanger, it is typically recommended that the design value of C_2 is restricted below 500, with the smaller the better. Furthermore, the gain effect obtained by decreasing C_2 is superior to C_1 under the same conditions.

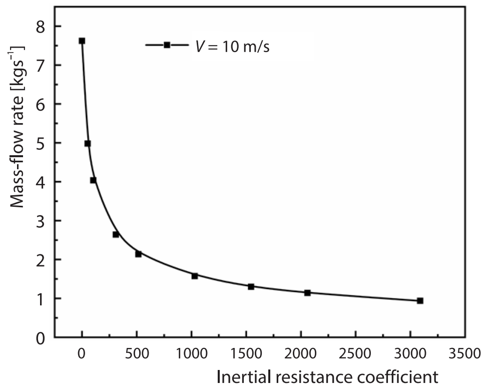

Figure 12. Variations the average naturally captured air volume with inertial resistance coefficient

Influence of core thickness on air captured capacity of the heat exchanger

Maintain the same altitude, C_1, and C_2, the influence of core thickness on the naturally captured air volume of the heat exchanger was studied.

As shown in fig. 13, on the whole, with the increase of core thickness, the air captured capacity also shows a downward trend. However, the downward trend is not significant. In addition, at the same core thickness, the average naturally captured air volume of the single heat exchanger increases with the increasing incoming wind velocity, showing a quasi-linear relationship. When the core thickness is 104 mm, the average naturally captured air volume of the single heat exchanger increases by approximately 1.18 kg/s for each increment in incoming wind velocity by 2.5 m/s. Compared with the core thickness of 94 mm, the naturally captured air volume decreases by 0.02 kg/s on average, with a reduction range of about 1.7%. Thus, it can be found the core thickness has a relatively slight effect on the naturally captured air volume of the heat exchanger. In order to ensure that C_1 and C_2 are within the recommended value range, the core thickness can be appropriately raised to effectively improve the heat transfer area of the heat exchanger.

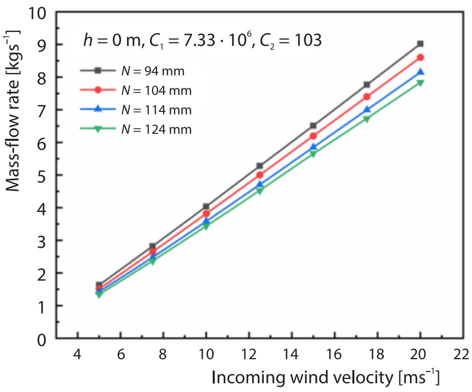

Figure 13. Variations of the average naturally captured air volume with incoming wind velocity at different core thickness

Conclusions

In this paper, a numerical model of the outside cabin heat exchanger of a 4.5 MW wind power generation was established. The influences of altitude, viscous resistance coefficient, inertial resistance coefficient, and core thickness on the naturally captured air volume of the heat exchanger were analyzed. The main conclusions are as follows.

- In this calculation model, the naturally captured air volume of the seven single heat exchangers tends to be larger on both sides and smaller in the middle, and there is a quasi-linear increase proportional to the incoming wind velocity.
- With different altitudes, the average naturally captured air volume of the heat exchanger reduces gradually with the increase of altitude. It is found that the reduction effect becomes obvious with the increase of incoming wind velocity.
- The average naturally captured air volume of the heat exchanger decreases with the increase of the C_1 and C_2. The decreasing range is increased as the incoming wind velocity increases. Meanwhile, it is discovered that when the design value of C_1 and C_2 should be restricted in the order of 10^6 and below 500, respectively, the air captured capacity of the heat exchanger is superior.
- The average naturally captured air volume of the heat exchanger reduces with the rise of core thickness. However, it is found that the effect of core thickness is slight. To ensure that C_1 and C_2 are within the recommended value range, the core thickness can be appropriately raised to improve the heat transfer area of the heat exchanger.

Nomenclature

a – fitting coefficient
b – fitting coefficient
C_1 – viscous resistance coefficient, [m^{-2}]
C_2 – inertial resistance coefficient, [m^{-1}]
C_{ij} – inertial loss coefficient matrix
D_{ij} – hiscous loss coefficient matrix
H – height of natural wind field, [m]
h – altitude, [m]
L – length of natural wind field, [m]
m – length of air side through, [mm]
N – heat exchanger core thickness, [m]
n – length of ethylene glycol side through, [mm]
Δn – porous media thickness, [mm]
ΔP – pressure drop, [Pa]
p – static pressure, [Pa]
S_i – momentum source term in the i^{th} direction, [kgm^{-2}s^{-2}]
u – velocity component of fluid, [ms^{-1}]
V – incoming wind velocity, [ms^{-1}]
x – space co-ordinate, [m]
W – width of natural wind field, [m]

Greek symbols

α – permeability, [m^2]
μ – dynamic viscosity coefficient, [Pa·s]
μ_{eff} – effective viscosity, [Pa·s]
ρ – density, [kgm^{-3}]

Subscripts

i – i^{th} direction
j – j^{th} direction

Acknowledgment

This work is supported by the Industry University Research Cooperation Project of Jiangsu (No. BY2020476), Postgraduate Practice Innovation Program of Jiangsu Province (No. SJCX21_1286).

References

[1] Patankar, S. V, Spalding, D. B, *Heat Exchanger Design Theory Source Book*, McGRAW-HiLL, New York, USA, 1974
[2] Ding, W., *et al*., Numerical Investigation of a Compact Tube Heat Exchanger for Hypersonic Pre-Cooled Aero-Engine, *Applied Thermal Engineering*, *170* (2020), 114977
[3] Kim, J., *et al*., Compound Porous Media Model for Simulation of Flat top U-Tube Compact Heat Exchanger, *International Journal of Heat and Mass Transfer*, *138* (2019), Aug., pp. 1029-1041
[4] Li, Z. Z., *et al*., An Approach Based on the Porous Media Model for Numerical Simulation of 3-D Finned-Tubes Heat Exchanger, *International Journal of Heat and Mass Transfer*, *173* (2021), 121226
[5] Zhao, B., *et al*., A Feasibility Analysis on Numerical Simulation of U-shaped Tube Bundle Heat Exchanger Using Dualmesh Method Coupled with Porous Media Model, *Heat Transfer Research*, *52* (2021), 2, pp. 75-95
[6] Vlahostergios, Z., *et al*., Effect of Turbulence Intensity on the Pressure Drop and Heat Transfer in a Staggered Tube Bundle Heat Exchanger, *Experimental Thermal and Fluid Science*, *60* (2015), Jan., pp. 75-82
[7] Guo, J. Z., *et al*., Performance Analysis of Automobile Heat Exchangers and Optimization of Fin Structure (in Chinese), *Science Technology and Engineering*, *16* (2016), 2-3, pp. 58-64
[8] Qu,T., *et al*., Multiscale Simulations of Fluid-flow for Finned Elliptic Tube Heat Exchangers Using Porous Media Approach, *Proceedings*, ASME 2014 International Mechanical Engineering Congress and Exposition, Montreal, Quebec, Canada, 2014, pp. 14-20
[9] Wang, W., *et al*., Numerical Study on Hydrodynamic Characteristics of Plate-Fin Heat Exchanger Using Porous Media Approach, *Computers and Chemical Engineering*, *61* (2014), Feb., pp. 30-37
[10] Du, J., Zhao, H. T., Numerical Simulation of a Plate-Fin Heat Exchanger with Offset Fins Using Porous Media Approach, *Heat and Mass Transfer*, *54* (2018), 3, pp. 745-755
[11] Zhang, Q., *et al*., Heat and Mass Transfer and Resistance Characteristics of Evaporative Air Cooler with High Finned-Tube Bundles, *Heat Transfer Research*, *49* (2018), 17, pp. 1705-1720
[12] Huang, Z. F., *et al*., Enhancing Heat Transfer in the Core Volume by Using Porous Medium Insert in a Tube, *International Journal of Heat and Mass Transfer*, *53* (2010), 5-6, pp. 1164-1174
[13] Missirlis,D., *et al*., Numerical Development of a Heat Transfer and Pressure Drop Porosity Model for a Heat Exchanger for Aero Engine Applications, *Applied Thermal Engineering*, *30* (2010), 11-12, pp. 1341-1350

[14] Mohammadi, M. H., et al., Thermal Optimization of Shell and Tube Heat Exchanger Using Porous Baffles, *Applied Thermal Engineering*, *170* (2020), 115005
[15] Qu., S. C., *et al*., Inned Tube Bundle Porous Media Model Establishment Method and Volume Field Simulation Based on CFD Simulation (in Chinese), *Chinese Journal of Applied Mechanice*, *37* (2020), 2, pp. 494- 499
[16] Yan, X., Simulation Analysis of a Certain Type of Unmanned Helicopter Heat Exchanger Based on Porous Media Model (in Chinese), *Helicopter Technology*, *206* (2020), 4, pp. 25-28
[17] Isilk, E., Tugan, V., Investigation of the Effect of Baffle Cut on Heat Transfer and Pressure Drop in Shell and Tube Heat Exchangers Using CFD, *Heat Transfer Research*, *52* (2021), 10, pp. 1-18
[18] Tang, L. H., *et al*., Air Inlet Angle Influence on the Air-Side Heat Transfer and Flow Friction Characteristics of a Finned Oval Tube Heat Exchanger, International Journal of Heat and Mass Transfer, *145* (2019), 118702
[19] Dovic, D., *et al*., Impact of Velocities and Geometry on Flow Components and Heat Transfer in Plate Heat Exchangers, *Applied Thermal Engineering*, *197* (2021), 117371
[20] Hadjadj, A., *et al.*, Air Velocity Effect on the Performance of Geothermal Helicoidally Water-Air Heat Exchanger under EI Oued Climate, Algeria, *Thermal Science and Engineering Progress*, *20* (2020), 100548
[21] Xu, X., *et al.*, Heat Transfer Simulation of Vehicle Heat Exchanger in Plateau Environment, *Journal of System Simulation*, *30* (2018), 8, pp, 3146-3153
[22] Amiri, L., *et al*., Estimating Pressure Drop and Ergun/Forchheimer Parameters of Flow Through Packed Bed of Spheres with Large Particle Diameters, *Powder Technology*, *356* (2019), Nov., pp. 310-324
[23] Koekemoer, A., Luckos, A., Effect of Material Type and Particle Size Distribution on Pressure Drop in Packed Beds of Large Particles: Extending the Ergun equation, *Fuel*, *158* (2015), Oct., pp. 232-238
[24] Lai, T. W., *et al*., Extension of Ergun Equation for the Calculation of the Volume Resistance in Porous Media with Higher Porosity and Open-Celled Structure-Science Direct, *Applied Thermal Engineering*, *173* (2020), 115262
[25] Tian, X. W., *et al.*, Volume Resistance Characteristics of Power-Law Fluid in Particle-Packed Porous Media (in Chinese), *Journal of Harbin Institute of Technology*, *49* (2017), 1, pp. 126-132

Paper submitted: January 23, 2022
Paper revised: March 22, 2022
Paper accepted: March 23, 2022